Spectrum and Reactivity of the Solvated Electron in the Ionic Liquid Methyltributylammonium Bis(trifluoromethylsulfonyl)imide†

James F. Wishart*,‡ and Pedatsur Neta§

Chemistry Department, Brookhaven National Laboratory, Upton, New York 11973-5000, and Physical and Chemical Properties Division, National Institute of Standards and Technology, Gaithersburg, Maryland, 20899-8381

Received: December 20, 2002; In Final Form: February 20, 2003

Fast pulse radiolysis transient absorption experiments were conducted on the ionic liquid methyltributylammonium bis(trifluoromethylsulfonyl)imide (R_4NNTf_2). The solvated electron was observed to have a very broad absorption band peaking around 1410 nm ($\epsilon = 2.2 \times 10^4$ L mol^{-1} cm^{-1}) and a radiolytic yield (G) of 0.7×10^{-7} mol J^{-1}. Dry electron capture by aromatic solutes, such as benzophenone and pyrene, is very efficient in R_4NNTf_2. Reactions of the solvated electron with the same compounds are diffusion limited, with rate constants of only $k \approx (1-2) \times 10^8$ L mol^{-1} s^{-1} due to the high viscosity of the ionic liquid.

Introduction

By virtue of their unique properties, room-temperature ionic liquids are rapidly finding new applications in chemical synthesis, separations chemistry, electrochemistry, and other areas.[1] New families of ionic liquids are being developed at a steady pace. In order to properly exploit the potential of these new solvents, traditional methods of chemical kinetics studies must be applied, and in some cases adapted, to the study of chemical reactivity in ionic liquids.

Pulse radiolysis is a particularly useful technique for the measurement of fast redox reactions and reactions of radicals and other energetic transient species.[2] Although the experimental methods of pulse radiolysis bear a resemblance to those of laser flash photolysis, they are different and complementary in one important respect. Whereas photolysis usually involves absorption of the photonic energy by specific chromophores, in radiolysis the energy of the ionizing radiation (γ rays or energetic particles) is deposited in the bulk of the material. Thus, the primary radiation chemistry of a solution is dominated by the solvent itself, be it water, organic, or an ionic liquid. For water, and to a lesser extent other conventional solvents, elegant methods have been developed to convert primary radiolytic species into specific intermediates for the study of many types of reactions. A similar knowledge base must be assembled for ionic liquids if the versatile methods of pulse radiolysis are to be applied to this exciting new area.

Furthermore, applications of ionic liquids to processes of the nuclear fuel cycle have been intensively studied, and several patents have been issued.[3] Since ionic liquids cannot evaporate or burn, and their melting points can be controlled by design, they may substantially improve the safety as well as performance of nuclear fuel and waste handling processes if they can be used as substitutes for volatile organic or aqueous systems. This can only be accomplished if the relevant ionic liquid(s) are sufficiently stable under exposure to high radiation doses. An investigation into the radiochemical stability of certain imidazolium ionic liquids has been conducted using product studies and microsecond time scale pulse radiolysis.[3] This approach can be substantially augmented by pico- and nanosecond observations of the primary radiolytic species and the dependence of their yields and reactivities on the composition of the ionic liquid.

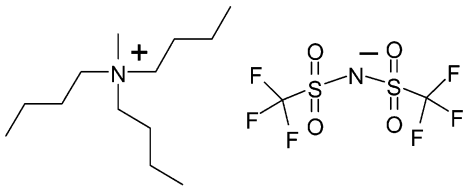

Figure 1. Methyltributylammonium bis(trifluoromethylsulfonyl)imide (R_4NNTf_2).

We have, therefore, set out to characterize the initial products of ionic liquid radiolysis and study their reactivity. The Brookhaven National Laboratory Laser-Electron Accelerator Facility (LEAF) pulse radiolysis system is designed to measure very fast reactions.[4] Earlier pulse radiolysis studies[3,5,6] conducted on slower time scales have investigated the reactions of secondary radicals and redox processes. The existence of a primary radiolytic species such as the solvated electron, however, has been inferred but not directly observed previously. The present work reports the solvated electron yield, spectrum, and reactivity toward certain solutes in the ionic liquid methyltributylammonium bis(trifluoromethylsulfonyl)imide (R_4NNTf_2, Figure 1).

Experimental Section[7]

Methyltributylammonium bis(trifluoromethylsulfonyl)imide was prepared by combining equimolar amounts of aqueous methyltributylammonium chloride ($MeBu_3N^+Cl^-$) and lithium bis(trifluoromethylsulfonyl)imide ($(CF_3SO_2)_2N^-Li^+$) solutions at room temperature. Both reagents were obtained from Aldrich. The viscous ionic liquid separated from the aqueous phase. The liquid was purified by repeated extractions with water to remove LiCl and excess reagent, and then dried under vacuum at 70 °C (yield 88%).

† Part of the special issue "Arnim Henglein Festschrift".

‡ Brookhaven National Laboratory. E-mail: wishart@bnl.gov.

§ National Institute of Standards and Technology. E-mail: pedi@email.nist.gov.

10.1021/jp027792z CCC: $25.00
Published on Web 04/05/2003

For initial investigation of the radiolytic behavior and transient spectra of neat R_4NNTf_2, the liquid was placed in a 2 cm path length cylindrical cell with a stem and Teflon stopcock. The contents of the cell were evacuated to ≈0.1 Pa (1 mTorr) with gentle warming (50 °C) for 20 min. After an initial burst of gas, no further degassing occurred. The cell was back-filled with argon for the radiolysis studies. For wavelengths where background absorption of the ionic liquid is significant ($\lambda \leq 400$ nm, $\lambda > 1050$ nm), the liquid was placed in a septum-capped, 1 cm spectrophotometer cuvette and sparged with argon for 10 min. The solvated electron lifetime observed when the sparging preparation method was used was the same as that found with the more rigorous evacuation procedure.

For the studies of reactions of solutes in R_4NNTf_2, standard cuvettes were used, one containing a control sample of neat solvent and up to four containing varying quantities of the desired solute. The solutes (pyrene, phenanthrene, benzophenone, or indole, all used as supplied by Aldrich) were weighed into clean and dry 1 cm Suprasil cuvettes (0.4−17 mg), and then a weighed amount of R_4NNTf_2 (typically 1.28 g, 1.03 mL) was added dropwise to the cuvette. The contents of the cuvettes were mixed and purged by bubbling with argon under gentle heat (50 °C) for at least 10 min.

Fast transient absorption pulse radiolysis experiments were carried out at the Brookhaven National Laboratory Laser-Electron Accelerator Facility (LEAF).[4] The LEAF RF photocathode electron accelerator was used to generate 8.7 MeV electron pulses of less than 150 ps duration. Radiolytic doses of 6−25 Gy were used. Analyzing light was provided by a pulsed xenon arc lamp. Narrow (10 nm) band-pass filters were used to select the analyzing wavelength; 40 nm-wide band-pass filters were used at wavelengths ≥1100 nm. Transient absorption signals were collected with FND-100 silicon (≤1050 nm) or GAP-500 InGaAs (≥900 nm) photodiodes, digitized with a Tektronix TDS-680B oscilloscope using custom software running on a DEC VAXstation 4000 computer. The data were analyzed with Igor Pro software (WaveMetrics, Inc., Lake Oswego, OR) using routines customized at BNL. The temperature for all experiments was 21 °C. Rate constants and molar absorption coefficients are reported with their estimated overall standard uncertainties, taking into account the standard deviation of the absorbance and kinetic measurements and estimated uncertainties in the values of the concentrations.

Results and Discussion

Primary Processes in Radiolysis. The general reaction scheme for radiolysis of a neat liquid (L) begins with the incident radiation (photon or particle) inducing excitations and ionizations of the constituent parts of the liquid.[2] (In the case of an ionic liquid, L represents the cations and anions, interchangeably.) Yields and reactivities of the excited species L* will be the subjects of subsequent investigations.

$$L \xrightarrow{\gamma \text{ or } e^-} L^*, L^{\bullet +} + e^-_{hot} \qquad (1)$$

The initially produced secondary electron in eq 1 (e^-_{hot}) carries some excess kinetic energy from the ionization event. It loses the excess energy through interactions with the solvent to come to rest at some distance from its starting point, which is now occupied by the electron-deficient species $L^{\bullet +}$, often called a hole. The electron is said to be thermalized when it has lost its excess kinetic energy (eq 2), but it is not considered to be solvated until the liquid has reorganized to an equilibrium configuration around the electron (eq 3), which may occur in more than one step. The precursor states to the solvated electron are often collectively called the "dry electron",[8,9] and we will use this term to refer to all such species (including e^-_{hot} and e^-_{th}).

$$e^-_{hot} \rightarrow e^-_{th} \qquad (2)$$

$$e^-_{th} \rightarrow \rightarrow \rightarrow e^-_{solv} \qquad (3)$$

Ionization events transfer a wide distribution of kinetic energies, which in turn results in a distribution of electron−hole thermalization distances. Depending on the electron−hole separation for a given pair and the effective dielectric constant of the liquid, the Coulombic potential inducing the pair to recombine may be less than the thermal energy *kT*. In this case, the electron and hole are free to diffuse apart and become "free ions" (from the perspective of molecular liquids). The distance at which the Coulombic potential is equal to *kT* is the well-known Onsager radius. Electron−hole pairs that thermalize at distances shorter than the Onsager radius will have a high probability to recombine. Consequently, free-ion yields are large in high-dielectric solvents such as water and small in hydrocarbons where few ion pairs thermalize at distances longer than the very large Onsager radii.

Dielectric constants of ionic liquids have not been reported to our knowledge, but spectroscopic measurements of solvatochromic probes[10,11] in ionic liquids have been used to estimate polarities on the $E_T(30)$ scale based on Reichardt's betaine dye.[11f] Ionic liquids containing imidazolium cations have E_T(30) values close to ethanol (51.9 kcal mol^{-1}, 217 kJ mol^{-1}), reflecting the hydrogen-bond donating ability of the C-2 carbon. Ionic liquids containing C-2 methylated imidazolium[11c] and tetraalkylammonium[11f,g] cations have lower $E_T(30)$ values in the 42−48 kcal mol^{-1} range. The peak wavelength of the intramolecular charge-transfer absorption band of Reichardt's betaine dye in R_4NNTf_2 is 612 nm, resulting in an $E_T(30)$ value of 46.7 kcal mol^{-1} (195 kJ mol^{-1}) close to the value of 45.6 kcal mol^{-1} observed in acetonitrile and more polar than those of benzonitrile and acetone (41.5 and 42.2 kcal mol^{-1}).[11f] Acetonitrile, benzonitrile, and acetone have Onsager radii of 1.5, 2.2, and 2.8 nm, respectively, compared to 0.7 nm in water, 2.3 nm in ethanol, and 30 nm in hexane.[12] In the absence of more direct evidence, polarity measurements suggest an approximate Onsager radius of 1.5 ± 0.3 nm for R_4NNTf_2.

Ionic liquids present a conceptual challenge to the conventional picture of ionization and recombination painted here, as well as to the applicability of continuum treatments. Despite their liquid state, neutron diffraction[13] and proton NMR[10] studies have shown that ionic liquids are disordered but reasonably regular ionic lattices. Coulombic screening should be effective at relatively short electron−hole pair separation distances, but the rate at which "hot" secondary electrons thermalize through interactions with the ionic lattice, and the resulting electron−hole pair distribution, are matters of significant uncertainty. Ionization of the liquid anion NTf_2^- will produce a neutral hole species $^{\bullet}NTf_2$ that can only recombine diffusively, not Coulombically, with the electron. These competing factors make a priori prediction of yields of free radical species and electrons very difficult.

Spectra and Lifetimes of the Initial Transients. Figure 2 shows representative pulse radiolysis kinetic traces of the neat, deoxygenated ionic liquid at 390, 650, and 900 nm. At wavelengths from 650 to 1050 nm, the traces can be accurately fit with a single first-order decay rate constant of 3.3×10^6 s^{-1}

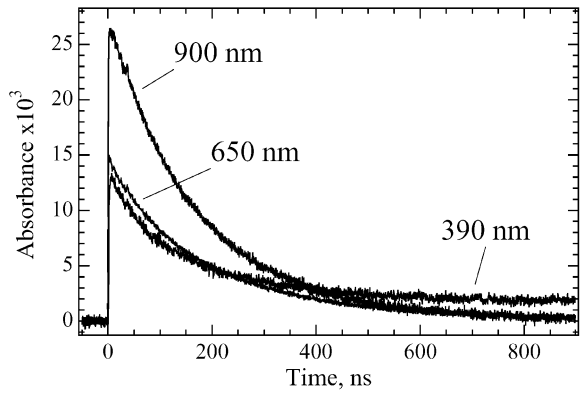

Figure 2. Absorbance traces for electron radiolysis of R_4NNTf_2 at (top to bottom) 900, 650, and 390 nm. Dose 12 Gy, path length 1 cm. Averages of three shots, except single shot at 900 nm.

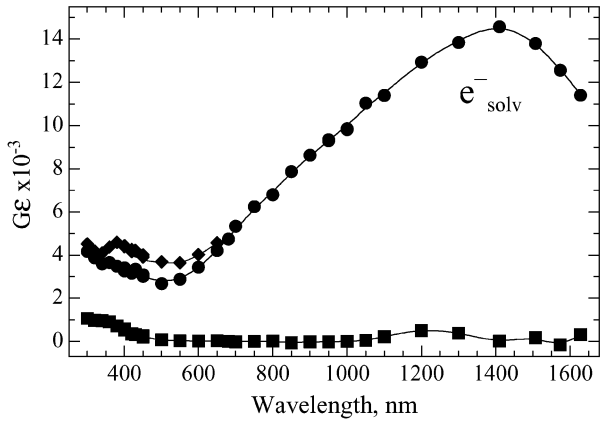

Figure 3. Transient spectra observed after electron radiolysis of R_4NNTf_2 as described in the text: species which decays with a 50 ns lifetime (◆) (to the level of ●); species with approximately 300 ns lifetime (●); residual absorbance at 1 μs (■). Dosimetry is referenced to the yield of $(SCN)_2^-$ in N_2O-saturated 10 mmol L^{-1} KSCN solution (6.1×10^{-7} mol J^{-1}), taking $\epsilon_{470} = 7950$ L mol^{-1} cm^{-1} and correcting by a factor of 1.16 for the difference in electron density between water and R_4NNTf_2.

(lifetime 300 ns).[14] At shorter wavelengths, an additional transient species with a decay rate constant of $(1.5-2.0) \times 10^7$ s^{-1} (lifetime 50 ns) is evident. The spectra shown in Figure 3 indicate the absorbance changes associated with the two transient species, as obtained from single- or double-exponential fits as appropriate in the range covered by the FND-100Q photodiode ($\leq$1050 nm), and the absorbance spectrum time slice between 20 and 30 ns measured by the GAP-500 photodiode at 900 nm and above.[15] Approximately 1 μs after the electron pulse, a slight residual absorbance persists around 400 nm. Comparison of the static UV−vis spectra of neat R_4NNTf_2 before and after repeated radiolytic pulses shows a buildup of a broad absorbance feature in the ultraviolet.

The small absorbance band that peaks at 400 nm and decays rapidly is assumed to correspond to electron-deficient species, such as the oxidized form of the solvent anion ($^\bullet NTf_2$) or cation ($R_4N^{\bullet 2+}$), but the exact identity has not been determined. These species probably are the precursors of fragment radicals, such as alkyl and trifluoromethyl radicals; the latter species has been discussed before.[5b,c]

The longer-lived transient species with peak absorbance around 1410 nm is assigned to the solvated electron by virtue of its spectrum and reactivity. As discussed later, this species reacts with aromatic acceptors to produce typical molecular anion spectra and also reacts with acids and dissolved O_2, but

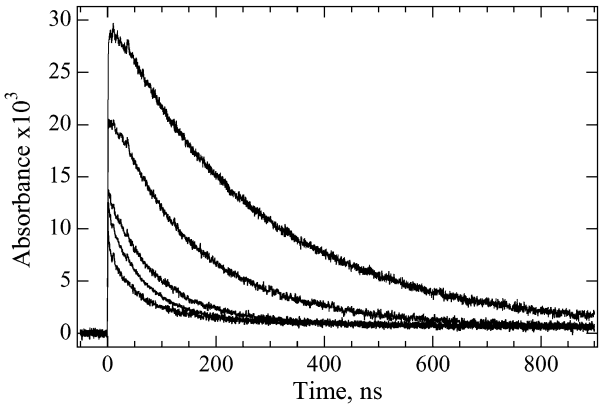

Figure 4. Absorbance vs time profiles at 900 nm for electron capture by (top to bottom) 0, 24, 48, 64, and 90 mmol L^{-1} benzophenone in R_4NNTf_2. Benzophenone radical anion absorbance is negligible. Dose 14 Gy, path length 1 cm.

does not react with the hole scavenger triethylamine. The electrochemical window of R_4NNTf_2 has been reported[16] to be +1.5 to −3 V versus Ag/Ag^+. The very negative cathodic limit indicates that the solvated electron is not readily scavenged by the solvent itself, and that it could exist as a discrete species in solution until it is scavenged. Since the electron decays via a simple first-order process, it must be reacting with impurities or with residual water (which may be present at levels up to 0.1%) rather than through a second-order process with a hole species.

A second absorbance feature associated with the solvated electron is apparent around 350 nm. By analogy to similar UV bands associated with the presence of the solvated electron in water[17] and amines,[18] this band is attributed to red-shifted transitions of the perturbed ionic solvent R_4NNTf_2 in the solvation shell surrounding the electron, as opposed to a direct excitation of the solvated electron.

At early times, kinetic traces in the NIR (800−1050 nm, see Figures 4 and 5a) show a small buildup of absorbance ($\tau \approx 4$ ns) before the solvated electron begins to decay. The most likely explanation for this phenomenon is a "blue" shift of the electron spectrum due to a slow solvent relaxation (solvation) process. At shorter wavelengths, a rise was not observed because of interference from the overlapping "hole" transient. Limited response of the InGaAs detector used at longer wavelengths did not allow observation of the spectral shift in the NIR.

The maximum of the solvated electron absorption spectrum in R_4NNTf_2 (1410 nm) occurs at much longer wavelengths than in water (715 nm) and alcohols (580−820 nm), but not as low energy as in ammonia (1850 nm) and simple alkylamines (1900−1950 nm).[19] Similar absorption maxima have been reported for alkyldiamines such as ethylenediamine, and 1,2- and 1,3-propanediamine (1360, 1500, and 1500 nm, respectively)[20,21] as well as acetonitrile (1450 nm).[19,22]

Electron Capture by Aromatic Acceptors. Four aromatic electron scavengers (benzophenone, pyrene, phenanthrene, and indole) were used to confirm the identity and examine the reactivity of the species assigned to be the solvated electron. Figures 4 and 5a show how the rate of solvated electron decay at 900 or 1030 nm increases with electron acceptor concentration in the cases of benzophenone and pyrene.

The first-order rate constants calculated from such traces for the four aromatic compounds show linear correlation with solute concentration (Figure 6), and the resulting second-order rate constants for solvated electron capture are given in Table 1.

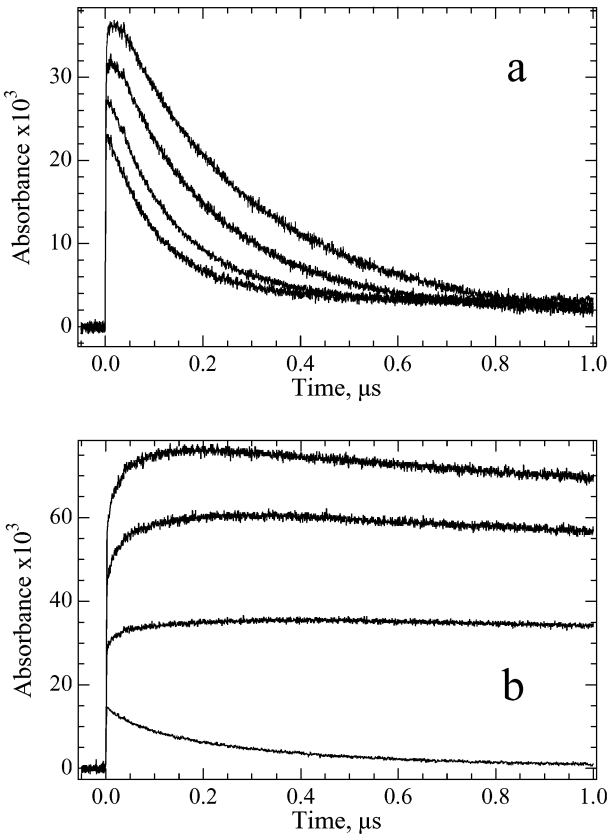

Figure 5. (a) Absorbance traces of solvated electron decay at 1030 nm for (top to bottom) 0, 8.3, 21, and 33 mmol L^{-1} pyrene in R_4NNTf_2. (b) Absorbance traces of pyrene anion growth at 490 nm for (bottom to top) 0, 8.3, 21, and 33 mmol L^{-1} pyrene in R_4NNTf_2. Averages of 2−4 runs, dose normalized to 15 Gy, 1 cm path length.

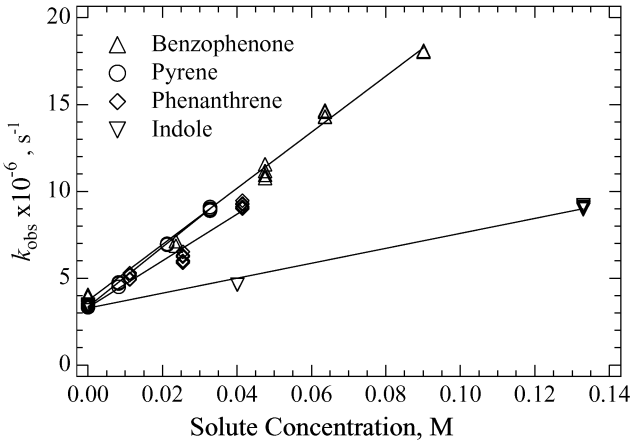

Figure 6. Plots of observed rate constants for solvated electron decay versus acceptor concentration for benzophenone, pyrene, phenanthrene, and indole in R_4NNTf_2.

Benzophenone, pyrene, and phenanthrene have similar rate constants, (1.3−1.7) × 10^8 L mol^{-1} s^{-1}, while the rate constant for the weaker electron acceptor indole is lower by a factor of 3. In water and alcohols, the first three solutes react with solvated electrons with diffusion-controlled rate constants, (1−3) × 10^{10} L mol^{-1} s^{-1} (based on actual measurements for benzophenone and by comparison with other polycyclic aromatics). We assume that the rate constants in the ionic liquid are also diffusion-controlled. The finding that the rate constants in the ionic liquid are about 2 orders of magnitude lower than those in water and alcohols is in line with the viscosity of R_4NNTf_2 being over 2 orders of magnitude higher than that of water and alcohols. Indole has a lower electron affinity than the other three compounds and is known to react with the hydrated electron with a rate constant of 2 × 10^8 L mol^{-1} s^{-1}. The reaction in water is much slower than the diffusion-controlled limit. The rate constant in the ionic liquid is also below the diffusion-controlled limit, but only by a factor of 5. This observation supports the contention that the rate constants for the reaction of the electron with pyrene, phenanthrene, and benzophenone are diffusion-limited.

TABLE 1: Rate Constants for Solvated Electron Capture and C_{37}/Q_{37} Values for Dry Electron Capture by Several Scavengers in R_4NNTf_2

scavenger	$k(e^-_{solv})$, L mol^{-1} s^{-1}	C_{37}, mol L^{-1} [a]	Q_{37}, L mol^{-1} [a]
benzophenone	(1.6 ± 0.1) × 10^8	0.062	16
pyrene	(1.7 ± 0.1) × 10^8	0.063	16
phenanthrene	(1.3 ± 0.1) × 10^8	0.084	12
indole	(4.3 ± 0.3) × 10^7	0.22	4.5
acid (as 70% $HClO_4$)	(6.2 ± 0.4) × 10^7	0.20	5.0
O_2	(1.1 ± 0.1) × $10^7/[O_2]_{sat}$	not obsd	

[a] The standard uncertainty of the C_{37} and Q_{37} values is 10%.

The rate constants for reaction of the solvated electron with pyrene, phenanthrene, and benzophenone, (1.3−1.7) × 10^8 L mol^{-1} s^{-1}, are similar to those determined by McLean et al.[23] for the quenching of triplet benzophenone by naphthalene in several butylmethylimidazolium ionic liquids, which were expected to be diffusion-controlled. The diffusion-controlled limit for R_4NNTf_2 was estimated from the measured viscosity and the equation $k_{diff} = 8000RT/3\eta$ to be ≈1.5 × 10^7 L mol^{-1} s^{-1}.[5b] McLean and co-workers also observed that their measured rate constants exceeded the limit estimated by this equation by an order of magnitude. It has been observed in several cases involving diffusion through viscous liquids and polymeric materials that the linearity implied by the equation does not hold and that the mobilities of molecules are higher than predicted.[24] These findings were interpreted by inferring that the microviscosity experienced by solutes was significantly lower than the macroviscosity of the medium, because the latter depends on movement of the entire solvent molecule whereas the former only requires movement of segments of solvent molecules and is affected by the amount of free volume in the solvent.

Dry Electron Capture. It is also evident from inspection of Figures 4 and 5a that the initial solvated electron yield decreases as the scavenger concentration is increased. This is due to scavenging of the dry electron by the solutes.[8,9,25−29] If the solute concentration is high enough, some fraction of the electrons produced by solvent ionization will be captured by solute molecules before the electrons can become fully solvated. The fractional yield of solvated electrons remaining after this process can be described as a function of the scavenger concentration by the following relation (eq 4), where G_c is the yield of solvated electrons at a given scavenger concentration c, G_0 is the yield in the absence of scavenger, and C_{37} is the concentration where only 1/e (37%) of the electrons survive to be solvated. Some authors prefer to use Q_{37} (=$1/C_{37}$) as a measure of the quenching efficiency, and both quantities are reported in Table 1.

$$G_c/G_0 = \exp(-c/C_{37}) \quad (4)$$

The values of Q_{37} reported in Table 1 for benzophenone, pyrene, and phenanthrene are large even when compared to those reported[25−29] for efficient dry electron scavengers in water,

ethanol, and 1-propanol (e.g., CCl_4 in EtOH[29] 7 L mol^{-1}, in PrOH[26] 7.7 L mol^{-1}; acetone in water[27,29] 0.7 L mol^{-1}, in EtOH[29] 3.3 L mol^{-1}, in PrOH[26,29] 4 L mol^{-1}; $Cr_2O_7^{2-}$ in water[27] 8.3 L mol^{-1}). There is a report of a comparably high Q_{37} value of about 20 L mol^{-1} ($C_{37} \approx 50$ mmol L^{-1}), for benzophenone in decanol,[30] and the value in ethanol is 7.1 L mol^{-1}.[29]

The relatively high dry electron scavenging efficiency found in this ionic liquid has several important implications. First, the high efficiency means that even a relatively low concentration of a solute may be enough to scavenge a significant fraction of the electrons, altering the radiation chemistry of the solution and modifying the yields of radiolysis products. Particular attention must be paid to the effects of dry electron scavenging on ionic liquid solutions of radioactive materials, where it may yield undesirable radiolysis products and accelerate the accumulation of solvent radiation damage. Second, efficient dry electron capture can be a boon to studies of ultrafast electron-transfer reactions because it may permit generation of the electron-transfer precursor state much faster than the diffusion-controlled reaction of the starting material with the solvated electron would allow. Finally, the results show that ionic liquids are a useful platform for testing proposed mechanisms for dry electron capture in other, molecular solvents. Some mechanisms postulate a competition between solvation and electron capture, which is a plausible explanation for our findings given the viscosity of 0.7 Pa s for R_4NNTf_2 and the spectroscopic evidence for slow solvation. Controlled design of ionic liquids allows detailed control over their solvation dynamics through viscosity and the presence or absence of functional groups. In further work, we will explore the relationship between ionic liquid solvation dynamics and dry electron capture.

Solvated Electron Yield. Dry electron capture by pyrene provides a convenient method to estimate the initial yield of the solvated electron in R_4NNTf_2, on the assumption that the spectral properties of the pyrene radical anion in the ionic liquid are similar to those in molecular solvents. The 490 nm absorbance peak of the pyrene radical anion is useful for this purpose because it is very intense, there is little interference from the radical cation, and the peak occurs at the same wavelength in R_4NNTf_2 as in other media.[31−33] Phenanthrene is not a good choice because of significant overlap of the radical anion and cation absorption bands over the accessible spectral region, and benzophenone is unsuitable because the peak wavelength of the radical anion absorption is solvent dependent.[34,35]

First-order kinetic fits of solvated electron decay at 1030 nm (Figure 5a) and pyrene anion growth at 490 nm (Figure 5b) were used to obtain extrapolated time-zero absorbance values for each of the four pyrene concentrations (0, 8.3, 21.3, 32.8 mmol L^{-1}). For each concentration, the extrapolated 490 nm value was plotted versus the corresponding 1030 nm value. The four points fit well to a line with slope -2.9 ± 0.1 (Supporting Information, Figure 1S). Using the reported extinction coefficient[31] of the pyrene anion (5.0×10^4 L mol^{-1} cm^{-1}) and correcting[36] for solvated electron absorbance at 490 nm, the extinction coefficient of the solvated electron in R_4NNTf_2 is 1.6×10^4 L mol^{-1} cm^{-1} at 1030 nm and the maximum extinction coefficient is 2.2×10^4 L mol^{-1} cm^{-1} at 1410 nm. The peak extinction coefficient is comparable to those observed[20] for the electron in ethylenediamine and propanediamine (2.0×10^4 to 2.2×10^4 L mol^{-1} cm^{-1}) in the same region. The extinction coefficient of the 1450 nm band of the solvated electron in acetonitrile was reported[37] to be 2.3×10^4 L mol^{-1} cm^{-1} although recent work[22] on the equilibrium between the solvated electron species responsible for the 1450 nm band and the anionic species associated with the absorption band at 530 nm suggests that the true 1450 nm extinction coefficient may be as large as 5.3×10^4 L mol^{-1} cm^{-1}.

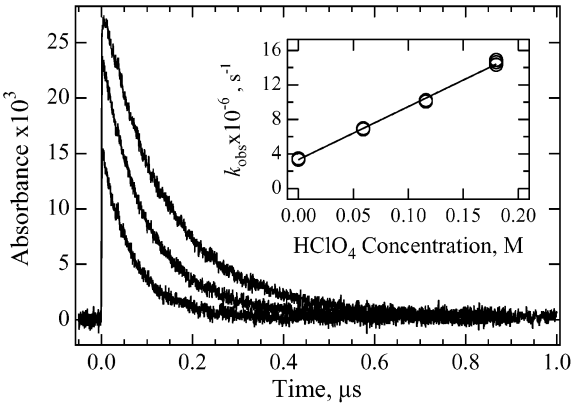

Figure 7. Absorbance traces at 1030 nm for the decay of the solvated electron in the presence of (top to bottom) 59, 116, and 180 mmol L^{-1} $HClO_4$ (added as 70% $HClO_4$) in argon-saturated R_4NNTf_2. Inset: plot of observed rate constant for electron decay at 1030 nm as a function of $HClO_4$ concentration.

The observed $G\epsilon$ value of 1.05×10^4 at 1030 nm in Figure 2b results in an estimated solvated electron yield (G) of $(0.7 \pm 0.05) \times 10^{-7}$ mol J^{-1} in R_4NNTf_2, extrapolated to time zero. This is a very interesting result which places the yield well below most polar solvents such as water, alcohols, and amines ($G = (2-3) \times 10^{-7}$ mol J^{-1}) but well above most hydrocarbons ($G = (0.05-0.33) \times 10^{-7}$ mol J^{-1}).[12,38] The solvated electron yield in R_4NNTf_2 is roughly the same as the aggregate G value for the materials used in nuclear fuel cycle processing, such as hydrocarbon/trialkyl phosphate mixtures. Ionic liquids may have processing and safety advantages which would make them good substitutes for the materials in use now, and this result indicates that the radiation stability of this ionic liquid is no worse than the media in current use.

Electron Scavenging by Acid. Solvated electron absorbance decay at 1030 nm was measured in the presence of three concentrations of perchloric acid (Figure 7). The solutions were prepared by the addition of concentrated perchloric acid (70% in water) to neat R_4NNTf_2, followed by 15 min of argon sparging. In the presence of the excess water carried with the acid (2.4 equiv of H_2O per $HClO_4$), the protonated species in this system may either be H_3O^+ or an equilibrium mixture of H_3O^+ and $HNTf_2$.[39] The absorbance traces show dry electron scavenging as indicated by decreasing initial solvated electron yields with increasing acid concentration. The values of C_{37} and Q_{37} derived from these data are 0.20 mol L^{-1} and 5.0 L mol^{-1}, respectively (Table 1). The second-order rate constant for the reaction of the solvated electron with the acid, obtained from a plot of the observed first-order decay rate constants versus acid concentration (Figure 7 inset), is $(6.2 \pm 0.4) \times 10^7$ L mol^{-1} s^{-1}. Both the Q_{37} and $k(e^-_{solv})$ values for the acid are comparable to those obtained for indole, and smaller than those of the other aromatic scavengers reported already. Lewis and Jonah[26] reported $Q_{37} = 3.2$ L mol^{-1} and $k(e^-_{solv}) = 1.0 \times 10^{10}$ L mol^{-1} s^{-1} for perchloric acid in *n*-propanol at 25 °C (viscosity 0.0019 Pa s).

Reaction of the Solvated Electron with Oxygen. The decay of the solvated electron absorption at 1030 nm is accelerated in changing from an argon-saturated R_4NNTf_2 solution to dry-air-saturated and oxygen-saturated solutions (Figure 8). Since the solubility of oxygen in this ionic liquid has not yet been

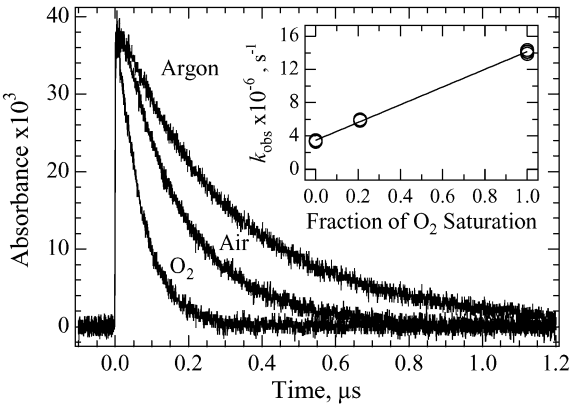

Figure 8. Absorbance traces for decay of the solvated electron in argon-, air-, and oxygen-saturated R_4NNTf_2 at 1030 nm. Inset: plot of observed rate constant for electron decay at 1030 nm as a function of oxygen saturation.

determined, the observed rate constants are plotted against the fraction of oxygen saturation (Figure 8 inset). The second-order rate constant derived from this plot can be expressed as $(1.1 \pm 0.1) \times 10^7/[O_2]_{sat}$ s^{-1}. If we assume that the solubility of oxygen in R_4NNTf_2 is in the same range as that reported for the ionic liquid $bmimPF_6$ (0.6 mmol L^{-1})[40] and for water (1.2 mmol L^{-1}), the rate constant for the solvated electron reaction with O_2 would be on the order of 1×10^{10} L mol^{-1} s^{-1}, much higher that the values for the aromatic compounds. This result implies that (a) the rate of diffusion for O_2 in R_4NNTf_2 is significantly higher than for the other solutes we have studied, or (b) the limiting solubility of O_2 in R_4NNTf_2 is considerably higher than 1 mmol L^{-1}, or both. Regarding case a, it is possible that a small, neutral molecule such as O_2 could be more mobile because it may diffuse easily among voids which occur in the ionic liquid due to poor packing. Regarding case b, it is very likely that the aliphatic and perfluorinated structural components of the R_4NNTf_2 increase the solubility of O_2 relative to that of water and $bmimPF_6$. The solubilities of O_2 in hydrocarbons are on the order of 10 mmol L^{-1}, and the solubilities in perfluorocarbons are a factor of 2−3 times higher than that.[41]

No dry electron scavenging by O_2 is observed in the experimental absorbance traces, which may be due to insufficient solubility of oxygen in this ionic liquid and/or a low scavenging efficiency (Q_{37}). Dry electron scavenging efficiency data for O_2 are not available in the literature due to its limited solubility in the liquids normally studied, such as water and alcohols.

Conclusion

Deposition of ionizing radiation in the ionic liquid R_4NNTf_2 leads to the production of solvated electrons that persist for hundreds of nanoseconds. The solvated electron reacts with benzophenone, pyrene, and phenanthrene with rate constants of $(1.3-1.7) \times 10^8$ L mol^{-1} s^{-1}, suggesting that this value is near the diffusion-controlled limit in this viscous ionic liquid. Indole and H_3O^+ react only slightly more slowly. The process of electron solvation is slow (about 4 ns) at room temperature, due at least in part to the viscosity of the solvent. Capture of presolvated, "dry" electrons by solutes is very efficient in R_4NNTf_2 compared to other solvents, perhaps because of less competition from the slower solvation process. The relationship between dry electron capture and electron solvation will be explored in further work.

The absorption spectrum of the solvated electron in R_4NNTf_2 has a maximum around 1410 nm, comparable to that observed for ethylenediamine. The radiolytic yield of solvated electrons is 0.7×10^{-7} mol J^{-1}, considerably lower than that in water and other polar solvents, but higher than most organic solvents. The results indicate that this ionic liquid will be a very useful medium for radiolytic studies of chemical reactivity, such as electron-transfer reactions.

Acknowledgment. The work performed at Brookhaven National Laboratory was funded under Contract DE-AC02-98CH10886 with the U.S. Department of Energy and supported by its Division of Chemical Sciences, Office of Basic Energy Sciences.

Supporting Information Available: Plot of the correlation between initial absorbances at 1030 and 490 nm for various pyrene concentrations. This material is available free of charge via the Internet at http://pubs.acs.org.

References and Notes

(1) (a) Welton, T. *Chem. Rev.* **1999**, *99*, 2071. (b) Wasserscheid, P.; Keim, W. *Angew. Chem., Int. Ed.* **2000**, *39*, 3772. (c) Earle, M. J.; Seddon, K. R. *Pure Appl. Chem.* **2000**, *70*, 1391. (d) Sheldon, R. *Chem. Commun.* **2001**, 2399−2407.

(2) (a) *Photochemistry and Radiation Chemistry: Complementary Methods for the Study of Electron Transfer*; Wishart, J. F., Nocera, D. G., Eds.; Advances in Chemistry Series 254; American Chemical Society: Washington, DC, 1998. (b) *Radiation Chemistry: Present Status and Future Trends*; Jonah, C. D., Rao, B. S. M., Eds.; Studies in Physical and Theoretical Chemistry 87; Elsevier Science: New York, 2001. (c) Mozumder, A. *Fundamentals of Radiation Chemistry*; Academic Press: San Diego, CA, 1999.

(3) Allen, D.; Baston, G.; Bradley, A.; Gorman, T.; Haile, A.; Hamblett, I.; Hatter, J. E.; Healey, M. J. F.; Hodgson, B.; Lewin, R.; Lovell, K. V.; Newton, B.; Pitner, W. R.; Rooney, D. W.; Sanders, D.; Seddon, K. R.; Sims, H. E.; Thied, R. C. *Green Chem.* **2002**, *4*, 152−158 and references therein.

(4) Wishart, J. F. In *Radiation Chemistry: Present Status and Future Trends*; Jonah, C. D., Rao, B. S. M., Eds.; Studies in Physical and Theoretical Chemistry 87; Elsevier Science: New York, 2001; Chapter 2, pp 21−35.

(5) (a) Behar, D.; Gonzalez, C.; Neta, P. *J. Phys. Chem. A* **2001**, *105*, 7607−7614. (b) Behar, D.; Neta, P.; Schultheisz, C. *J. Phys. Chem. A* **2002**, *106*, 3139−3147. (c) Grodkowski, J.; Neta, P. *J. Phys. Chem. A* **2002**, *106*, 5468−5473. (d) Grodkowski, J.; Neta, P. *J. Phys. Chem. A* **2002**, *106*, 9030−9035. (e) Grodkowski, J.; Neta, P. *J. Phys. Chem. A* **2002**, *106*, 11130−11134.

(6) Marcinek, A.; Zielonka, J.; Gebicki, J.; Gordon, C. M.; Dunkin, I. R. *J. Phys. Chem. A* **2001**, *105*, 9305−9309.

(7) The mention of commercial equipment or material does not imply recognition or endorsement by the National Institute of Standards and Technology, nor does it imply that the materials or equipment identified are necessarily the best available for the purpose.

(8) (a) Hamill, W. H. *J. Phys. Chem.* **1969**, *73*, 1341. (b) Sawai, T.; Hamill, W. H. *J. Chem. Phys.* **1970**, *53*, 3843.

(9) Wolff, R. K.; Bronskill, M. J.; Hunt, J. W. *J. Chem. Phys.* **1970**, *53*, 4211−4215.

(10) Bonhôte, P.; Dias, A.-P.; Papageorgiou, N.; Kalyanasundaram, K.; Grätzel, M. *Inorg. Chem.* **1996,** *35*, 1168−1178.

(11) (a) Carmichael, A. J.; Seddon, K. R. *J. Phys. Org. Chem.* **2000**, *13*, 591. (b) Aki, S. N. V. K.; Brennecke, J. F.; Samanta, A. *J. Chem. Soc., Chem. Commun.* **2001**, 413−414. (c) Muldoon, M. J.; Gordon, C. M.; Dunkin, I. R. *J. Chem. Soc., Perkin Trans. 2* **2001**, 433−435. (d) Fletcher, K. A.; Storey, I. A.; Hendricks, A. E.; Pandey, S.; Pandey, S. *Green Chem.* **2001**, *3*, 210−215. (e) Baker, S. N.; Baker, G. A.; Bright, F. V. *Green Chem.* **2001**, *3*, 210−215. (f) Reichardt, C. *Chem. Rev.* **1994**, *94*, 2319−2358. (g) Bart, E.; Meltsin, A.; Huppert, D. *J. Phys. Chem.* **1994**, *98*, 3295−3299.

(12) Swallow, A. J. In *Radiation Chemistry: Principles and Applications*; Farhataziz; Rodgers, M. A. J., Eds.; VCH: New York, 1987; pp 351−375.

(13) Hardacre, C.; Holbrey, J. D.; McMath, S. E. J.; Bowron, D. T.; Soper, A. K. *J. Chem. Phys.* **2003**, *118*, 273−278.

(14) In certain ionic liquid preparations, the decay rate constant was higher (up to 5.9×10^6 s^{-1}) presumably due to impurities. This variability can be seen when the 900 nm traces in Figures 2 and 4 are compared.

(15) There is a significant secondary response distortion of the transient absorption signal detected by the GAP-500 InGaAs diode, which reduces the peak absorbance signal observed in the decay of the solvated electron. This effect has been reported in detail by Cline et al.[15a] The effect of

thedistortion is uniform at wavelengths of 900 nm and longer. Therefore, the absorbance values from a time slice from 20 to 30 ns obtained with the GAP-500 were empirically scaled to overlap with the FND-100Q data at 900−1000 nm in order to construct the spectrum over the full wavelength range. (a) Cline, J. A.; Jonah, C. D.; Bartels, D. M. *Rev. Sci. Instrum.* **2002**, *73*, 3908−3915.

(16) Quinn, B. M.; Ding, Z.; Moulton, R.; Bard, A. J. *Langmuir* **2002**, *18*, 1734−1742.

(17) Nielsen, S. O.; Michael, B. D.; Hart, E. J. *J. Phys. Chem.* **1976**, *80*, 2482.

(18) Belloni, J.; Billiau, F.; Saito, E. *Nouv. J. Chim.* **1979**, *3*, 157−161.

(19) Belloni, J.; Marignier, J. L. *Radiat. Phys. Chem.* **1989**, *34*, 157−171.

(20) Dorfman, L. M.; Gavlas, J. F. In *Radiation Research. Biomedical, Chemical and Physical Perspectives*; Nygaard, O. F., Adler, H. J., Sinclair, W. K., Eds.; Academic Press: New York, 1975; pp 326−332.

(21) Gavlas, J. F.; Jou, F. Y.; Dorfman, L. M. *J. Phys. Chem.* **1974**, *78*, 2631−2635.

(22) Shkrob, I. A.; Sauer, M. C., Jr. *J. Phys. Chem. A* **2002**, *106*, 9120−9131.

(23) McLean, A. J.; Muldoon, M. J.; Gordon, C. M.; Dunkin, I. R. *Chem. Commun.* **2002**, 1880−1881.

(24) (a) Chu, D. Y.; Thomas, J. K. *J. Phys. Chem.* **1989**, *93*, 6250−6257. (b) Chu, D. Y.; Thomas, J. K. *Macromolecules* **1990**, *23*, 2217−2222. (c) Schmidt, W. F.; Holroyd, R. A. *Radiat. Phys. Chem.* **1992**, *39*, 349−353.

(25) Jonah, C. D.; Miller, J. R.; Matheson, M. S. *J. Phys. Chem.* **1977**, *81*, 1618−1622.

(26) Lewis, M. A.; Jonah, C. D. *J. Phys. Chem.* **1986**, *90*, 5367−5372.

(27) Jonah, C. D.; Bartels, D. M.; Chernovitz, A. C. *Radiat. Phys. Chem.* **1989**, *34*, 146−156.

(28) Glezen, M. M.; Chernovitz, A. C.; Jonah, C. D. *J. Phys. Chem.* **1992**, *96*, 5180−5183.

(29) Lam, K. Y.; Hunt, J. W. *Int. J. Radiat. Phys. Chem.* **1975**, *7*, 317−338.

(30) Lin, Y.; Jonah, C. D. *J. Phys. Chem.* **1993,** *97*, 295−302.

(31) Gill, D.; Jagur-Grodzinski, J.; Szwarc, M. *Trans. Faraday Soc.* **1964**, *60*, 1424−1431.

(32) Shaede, E. A.; Kurihara, H.; Dorfman, L. M. *Int. J. Radiat. Phys. Chem.* **1974**, *6*, 47−54.

(33) Kira, A.; Imamura, M.; Shida, T. *J. Phys. Chem.* **1976**, *80*, 1445−1448.

(34) Shida, T. *Electronic Absorption Spectra of Radical Ions*; Elsevier Science Publishers B.V.: Amsterdam, 1988.

(35) (a) Dainton, F. S.; Kemp, T. J.; Salmon, G. A.; Keene, J. P. *Nature* **1964**, *203*, 1050. (b) Scholes, G.; Simic, M.; Adams, G. E.; Boag, J. W.; Michael, B. D. *Nature* **1964**, *204*, 1187. (c) Keene, J. P.; Kemp, T. J.; Salmon, G. A. *Proc. R. Soc. London, Ser. A* **1965**, *287*, 494. (d) Keene, J. P.; Land, E. J.; Swallow, A. J. *J. Am. Chem. Soc.* **1965**, *87*, 5284. (e) Baxendale, J. H.; Fielden, E. M.; Keene, J. P. *Science* **1965**, *148*, 637. (f) Beaumond, D.; Rodgers, M. A. J. *Trans. Faraday Soc.* **1969**, *65*, 2973. (g) Wagner-Czauderna, E.; Kalinowski, M. K. *Collect. Czech. Chem. Commun.* **2000**, *65*, 1573−1579.

(36) The slope of the fitted line in Supporting Information Figure S1 (−2.9) corresponds to the following ratio: $\Delta A_{490}/\Delta A_{1000} = (\epsilon_{pyrene,490} - \epsilon_{elec,490})/(\epsilon_{pyrene,1030} - \epsilon_{elec,1030})$. If the absorbance of the pyrene anion at 1030 nm is assumed to be negligible ($\epsilon_{pyrene,1030} \approx 0$), the equation simplifies to $\Delta A_{490}/\Delta A_{1000} = (\epsilon_{pyrene,490} - \epsilon_{elec,490})/\epsilon_{elec,1030}$, and the ratio of solvated electron absorbance ($G\epsilon_{elec,490}/G\epsilon_{elec,1030} = 2840/10500$, interpolated values) can be obtained from Figure 3 to solve for $\epsilon_{elec,1030} = 15\,600\ M^{-1}\ cm^{-1}$.

(37) Bell, I. P.; Rodgers, M. A. J.; Burrows, H. D. *J. Chem. Soc., Faraday Trans. 1* **1977**, *73*, 315−326.

(38) Holroyd, R. A. In *Radiation Chemistry: Principles and Applications*; Farhataziz; Rodgers, M. A. J., Eds.; VCH New York, 1987; pp 201−235.

(39) $HNTf_2$ has been reported to be a very strong acid in the gas phase (Koppel, I. A.; Taft, R. W.; Anvia, F.; Zhu, S.-Z.; Hu, L.-Q.; Sung, K.-S.; DesMarteau, D. D.; Yagupolskii, L. M.; Yagupolskii, Y. L.; Ignat'ev, N. V.; Kondratenko, N. V.; Volkonskii, A. Y.; Vlasov, V. M.; Notario, R.; Maria, P.-C. *J. Am. Chem. Soc.* **1994**, *116*, 3047−3057), but in water it has $pK_a = 1.7$ (Foropoulos, J., Jr.; DesMarteau D. D. *Inorg. Chem.* **1984**, *23*, 3720−3723) and is a weaker acid than $HClO_4$.

(40) Anthony, J. L.; Maginn, E. J.; Brennecke, J. F. *J. Phys. Chem. B* **2002**, *106*, 7315−7320.

(41) Fogg, P. G. T.; Gerrard, W. *Solubility of Gases in Liquids*; Wiley: New York, 1991.